Spatiotemporal propagation dynamics of intense optical pulses in loosely confined gas-filled hollow-core fibers

Rui-rui Zhao(赵睿睿)[1,2], Ding Wang(王丁)[1,†], Zhi-yuan Huang(黄志远)[1], Yu-xin Leng(冷雨欣)[1,‡], and Ru-xin Li(李儒新)[1]

[1] *State Key Laboratory of High Field Laser Physics, Shanghai Institute of Optics and Fine Mechanics, Chinese Academy of Sciences, Shanghai* 201800, *China*
[2] *University of Chinese Academy of Sciences, Beijing* 100049, *China*

(Received 22 August 2016; revised manuscript received 18 September 2016; published online 30 November 2016)

We numerically study the propagation dynamics of intense optical pulses in gas-filled hollow-core fibers (HCFs). The spatiotemporal dynamics of the pulses show a transition from tightly confined to loosely confined characteristics as the fiber core is increased, which manifests as a deterioration in the spatiotemporal uniformity of the beam. It is found that using the gas pressure gradient does not enhance the beam quality in large-core HCFs, while inducing a positive chirp in the pulse to lower the peak power can improve the beam quality. This indicates that the self-focusing effect in the HCFs is the main driving force for the propagation dynamics. It also suggests that pulses at longer wavelengths are more suitable for HCFs with large cores because of the lower critical power of self-focusing, which is justified by the numerical simulations. These results will benefit the generation of energetic few-cycle pulses in large-core HCFs.

Keywords: spatiotemporal dynamics, hollow-core fiber, longer wavelengths

PACS: 42.65.Re, 42.65.Jx, 42.81.Qb **DOI:** 10.1088/1674-1056/26/1/014208

1. Introduction

Gas-filled hollow-core fibers (HCFs) have become an established pulse compressor for the generation of the intense few-cycle pulses used in high field laser physics and attosecond science.[1,2] This technique was originally demonstrated in an HCF with a 140 μm bore, where input pulses of 140 fs duration were compressed down to 10 fs.[3] The maximum pulse energy injected in the HCF is limited by the strong ionization of the gas at the fiber inlet, which results in a poor beam quality. To achieve the higher pulse energies required by the scientific community, methods using gas pressure-gradient,[4] circular polarized input pulse,[5] chirped input pulse,[6] larger fiber inner diameter,[7] planar or multi-core fibers,[8,9] and divided pulse nonlinear compression[10,11] have been proposed. Note that these methods can be combined to further improve the compressed pulse energy. Among these methods, the use of HCFs with larger cores is particularly straightforward. As a result, the inner diameter used has become larger and larger, with the current record being 1000 μm.[12] The question arises as to the upper limit of the fiber cores. Although there has been research into the optimal compressor design, and the lower limit of the fiber core is determined by the onset of ionization at the fiber input,[13] the upper limit of the fiber core has not been clearly defined. The use of large-core HCFs faces a number of problems, such as self-focusing and filamentation in the HCF due to higher pulse powers.[14,15] Some researchers are exploring ionization and plasma effects in HCFs for pulse compression,[16] but in the traditional implementation, self-phase modulation (SPM) is the main effect for spectral broadening.

In the past decade, the interest in obtaining few-cycle intense pulses at wavelengths longer than 800 nm has grown, particularly regarding the mid-IR range. Although optical parametric chirped pulse amplification is a promising method of delivering such pulses,[17] compressors based on HCF are still good choices in many cases. Granados *et al*. studied the wavelength scaling of optimal HCF designs.[18] Their results show that, as the fiber core diameter increases, the beam quality deteriorates. This indicates an upper limit for the fiber core if more than 85% of the pulse energy should be in the funamental mode, and as a result, the input pulse energy is limited to less than 2 mJ at 800 nm.

A recent study on the scale-invariance of nonlinear pulse propagation in free-space identified the scaling principles for larger geometries, higher pulse energies, and longer propagation distances.[19] The results are promising in the cases of filamentation and high-harmonic generation. Nonlinear propagation in HCFs is similar to that in free space. There is also a self-focusing effect, ionization loss, and plasma defocusing in HCFs when the pulse energy is sufficiently high. Filamentation in free space for pulse compression has been proposed and demonstrated experimentally. This has the advantage of higher energy efficiency compared with HCFs.[20] Unfortunately, when the pulse energy is higher, multifilamentation occurs and the beam quality is destroyed.[21] With proper scaling, a single filament can be preserved at high energy.[19] However, this requires a very delicate control over the beam param-

†Corresponding author. E-mail: wangding@siom.ac.cn
‡Corresponding author. E-mail: lengyuxin@mail.siom.ac.cn

eters before filamentation. If similar scaling principles could be identified in HCFs, the energy of the compressed pulse may be increased with good beam quality because of the mode discrimination effect of the waveguide structure. However, the similar scaling of propagation in gas-filled HCFs is difficult because of the nonlinear dependence of the various effects on the fiber geometry, i.e., the size of the inner diameter. Moreover, when the fiber core becomes sufficiently large, there will be a transition from guided propagation to free-space propagation due to the weakening of the waveguide influence. Thus, the advantage of using a waveguide disappears.

Although it faces a number of problems, the use of HCFs with larger cores is a tempting proposition for acquiring higher pulse energies. Therefore, the understanding of the propagation dynamics in such loosely confined waveguides is important and beneficial. In this paper, we theoretically study the nonlinear spatiotemporal propagation of intense optical pulses in gas-filled HCFs with different inner diameters. As the diameter increases, the propagation dynamics transit from tightly confined to loosely confined characteristics. In the tightly confined regime, most of the pulse energy is in the fundamental mode and the spatiotemporal distribution is uniform, whereas in the loosely confined regime, the spatiotemporal distribution is non-uniform and has considerable energy in high-order modes. To improve the beam quality, we also examine the gas pressure-gradient method and induce a positive chirp in the input pulse. It is found that the gas pressure gradient alone cannot improve the beam quality. However, inducing a positive chirp results in more output energy in the fundamental mode. The wavelength dependence of the propagation dynamics is also studied. The remainder of this paper is organized as follows. In Section 2, the theoretical model is introduced. Section 3 presents simulation results for the propagation of pulses centered at 800 nm in HCFs with different diameters. Section 4 discusses the wavelength dependence. The paper ends with our conclusions in Section 5.

2. Theoretical model

The propagation dynamics of optical pulses in HCFs is modeled by the waveguide version of the unidirectional pulse propagation equation (UPPE), which is described as follows:[22]

$$\begin{aligned}\partial_z U_{\rm m}(\omega,z) =& -\frac{\alpha_{\rm m}}{2}U_{\rm m}+{\rm i}\left(\beta_{\rm m}-\frac{\omega}{v_{\rm g}}\right)U_{\rm m}\\&+\frac{\omega}{c^2\beta_{\rm m}(\omega)\cdot 2a^2\int_0^1 r{\rm d}rJ_0^2(u_{\rm m}r)}\boldsymbol{e}_s\\&\times\int_0^a J_0(u_{\rm m}r/a)\left[{\rm i}\omega\frac{\boldsymbol{P}(r,\omega)}{\varepsilon_0}-\frac{\boldsymbol{j}(r,\omega)}{\varepsilon_0}\right]r{\rm d}r,\end{aligned}\quad(1)$$

where $U_{\rm m}$ is the fiber mode field; the subscript m indicates the fiber mode order; $\alpha_{\rm m}$ and $\beta_{\rm m}$ are the linear attenuation and dispersion of the fiber mode, respectively;[23] $v_{\rm g}$ is the group velocity of the fundamental mode at the central wavelength of the pulse; $J_0(u_{\rm m}r/a)$ describes the mode field distribution and is a zero-order Bessel function of the first kind; $u_{\rm m}$ is the m-th zero point of $J_0(x)$; ω, a, c, and ε_0 are the angular frequency, fiber inner radius, light speed, and permittivity in a vacuum, respectively; $P(r,\omega)$ and $j(r,\omega)$ describe the nonlinear polarization and plasma effects, respectively. The pulse electric field in the time domain can be reconstructed according to

$$E(x,y,z,t)=2\cdot{\rm Re}\left\{{\rm FFT}^{-1}\left[\sum\nolimits_{\rm m}U_{\rm m}(\omega,z)\times J_0(u_{\rm m}r/a)\right]\right\},\quad(2)$$

where ${\rm Re}\{\cdots\}$ indicates the real part of a quantity; ${\rm FFT}^{-1}$ is the inverse Fourier transform. $|E|^2$ is normalized according to the optical intensity. For the cubic Kerr effect, the nonlinear polarization is $P/\varepsilon_0=2n_0n_2\mathcal{I}E$, where $\mathcal{I}$ is the optical pulse intensity envelope. The gas ionization effect in the time domain is modeled by $j(t)/\varepsilon_0=cn_0W(\mathcal{I})U_{\rm i}(\rho_{\rm nt}-\rho)E/\mathcal{I}$, where $W(\mathcal{I})$ is the ionization rate calculated according to the PPT model;[24] $U_{\rm i}$ is the ionization potential; ρ is the electron density; and $\rho_{\rm nt}$ is the neutral density of the gas. The plasma effect in the frequency domain is modeled by

$$j(\omega)/\varepsilon_0=\frac{\tau_{\rm c}(1+{\rm i}\omega\tau_{\rm c})}{1+\omega^2\tau_{\rm c}^2}\frac{e^2}{\varepsilon_0 m_{\rm e}}{\rm FFT}[\rho E],$$

where e, $m_{\rm e}$, and $\tau_{\rm c}$ are the electron charge, mass, and collision time, respectively. Note that the ionization rate obtained with the PPT model is higher than that with the ADK model,[25] so the simulation results will be different from those using the ADK rates. However, the qualitative behavior is the same. Assuming the electrons are born at rest, the electron density ρ evolves as

$$\partial_t\rho=W(\mathcal{I})(\rho_{\rm nt}-\rho)+\sigma\mathcal{I}\rho/U_{\rm i},\quad(3)$$

where σ is the impact ionization cross-section.

Equation (1) is integrated using the fourth-order Runge–Kutta method with a self-adaptive step length and error control. The input pulses are of Gaussian type and are assumed to couple optimally into the fiber, i.e., with 98% pulse energy coupled to the fundamental mode. The pulses are decomposed into 15–20 modes, which ensures the convergence of the results.

To facilitate the data analysis, we define a Q factor as the ratio of the energy of the fundamental mode to the pulse energy.[18]

3. Simulation results

HCFs of diameter 250 μm are widely used for compressing pulses from Ti:Sa laser systems.[26] We first simulated a 0.5 mJ/40 fs/800 nm pulse propagating in a 250 μm diameter and 1 m long HCF filled with 300 mbar argon for comparison, as the typical experimental conditions. The inner diameter of the HCF was then increased to 500 μm, 1 mm, and 1.5 mm.

The pulse energies were scaled to 2 mJ, 8 mJ, and 18 mJ, respectively, to keep the input peak intensity unchanged. All other parameters were kept the same. Larger diameters were not explored, because 1.5 mm HCF already has no dominating mode, so further increasing the diameter would result in similar propagation dynamics. Note that the input peak intensity is a little higher than the value recommended in a previous study.[13] Although the peak intensity does not change, the peak powers scale quadratically with the fiber diameters, leading to a high degree of spatiotemporal coupling.

Figure 1 shows the evolution of the normalized pulse energies for different fiber modes in HCFs of different diameters. It can be seen that the pulse energy in 250 μm HCF decreases smoothly with a slower attenuation speed. The peak input power is 12.5 GW, far less than the critical power for self-focusing P_{cr} (108.2 GW). Therefore, the energy transferred from the fundamental mode to high-order modes is limited. Before 50 cm, there is a little oscillation between the fundamental mode and the high-order modes; after that, the total power of the pulse is sufficiently low that negligible power is fed to high-order modes through nonlinear effects. As a result, the waveguide filters most of the high-order modes, leaving only the fundamental and the second-order modes. In the whole process, the Q factor is above 0.85. This is characteristic of waveguide-confined propagation. For 500 μm HCF, the effect of mode discrimination is weak. Moreover, the peak power increases to 50 GW, about half of P_{cr}. As shown in Fig. 1, the energy exchange between different modes occurs at a larger magnitude over a larger periodicity before 50 cm compared with the 250 μm HCF. In the last 30 cm, the third-order mode also maintains a significant level of energy. The Q factor decreases to about 0.55 after 1 m propagation. When the inner diameter is increased to 1 mm, more high-order modes are excited to a significant level. The final Q factor decreases to about 0.3. In the 1.5 mm HCF, the fundamental mode is 'buried' in high-order modes after a quick drop. The corresponding Q factor is similar to that of the 1 mm HCF. As a result, further increases in the HCF diameter would result in similar propagation dynamics. Note that the transmission efficiency decreases with the diameter. This is due to the self-focusing induced ionization and high-order mode attenuation.

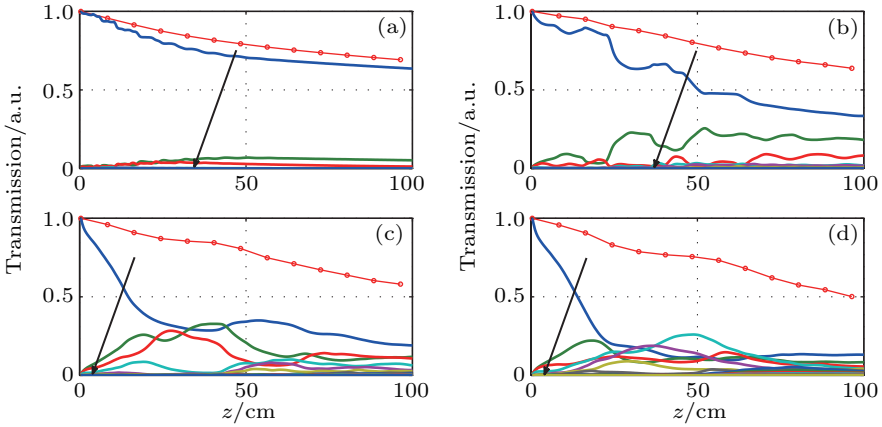

Fig. 1. (color online) Evolutions of normalized energies of the pulse (red-dotted lines) and different fiber modes (solid lines with various colors represent different fiber mode orders m of Eq. (1)) in the hollow-core fibers with (a) 250 μm, (b) 500 μm, (c) 1 mm, and (d) 1.5 mm diameters.

Figure 2 shows the transverse energy distribution in the four HCFs. A transition from tightly confined to loosely confined propagation dynamics can be seen. In the 250 μm HCF, the waveguide filters most of the high-order modes, allowing the transverse distribution to become stable and smooth over the last 40 cm. In the 1 mm and 1.5 mm HCFs, the transverse distributions exhibit considerable irregularity. There are two reasons for this irregularity. First, in the simulations, the peak intensity of the input pulse remained the same while the beam size was scaled with the inner diameter of the HCF to meet the optimal waveguide coupling condition. As a result, the peak power of the pulse increases, leading to stronger self-focusing effects. This results in the excitation of many high-order modes. Second, with the increase in the fiber diameter, the attenuation of the high-order modes is weakened significantly. The resulting mixing of many high-order modes with the fundamental mode leads to an irregular transverse distribution. It is interesting to see that, in the first 20 cm, the beam size does not contract because of self-focusing, which is different from propagation in free space. This difference suggests that although the waveguide confinement is very weak, it still influences the propagation dynamics. The 500 μm HCF is in the intermediate regime.

Figure 3 shows the spatiotemporal intensity distribution at the outlet of the HCFs after proper chirp compensation. The intensity envelope for the 250 μm HCF is uniform in the spatial domain, and there is a main peak of 5.428 fs full-width half-maximum (FWHM), which is ideal for later experiments. The pulse envelope in the 500 μm HCF is also acceptable, as there is a dominant peak. However, for the 1 mm and 1.5 mm HCFs, the pulse splits in both the temporal and spatial domains. According to Fig. 1, this is because more than five modes are excited and there is no dominant mode.

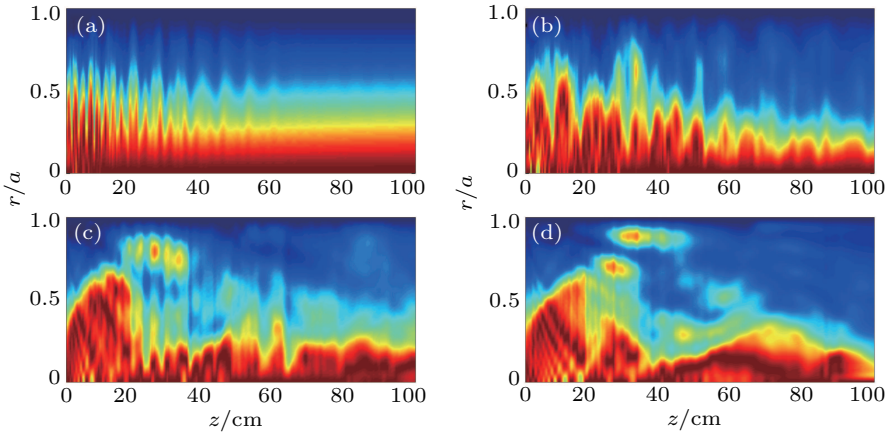

Fig. 2. (color online) Transverse energy distributions in the hollow-core fibers with (a) 250 μm, (b) 500 μm, (c) 1 mm, and (d) 1.5 mm diameters.

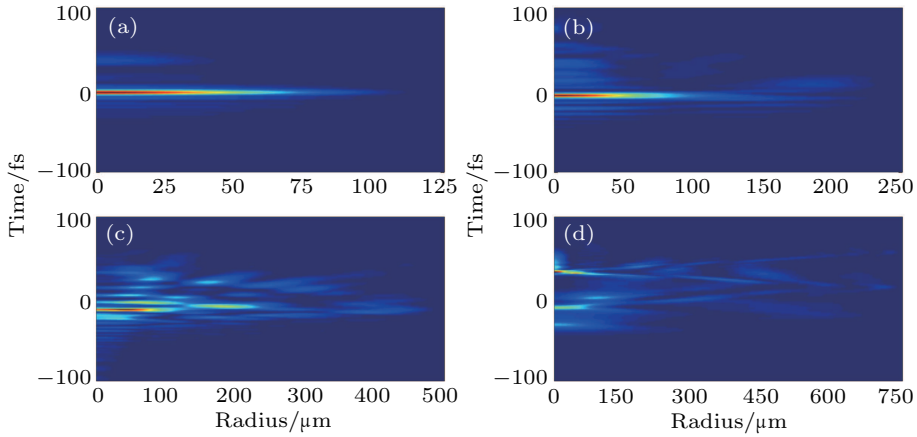

Fig. 3. (color online) Spatiotemporal intensity distributions of the pulses with proper chirp compensations after 1 m propagation in the hollow-core fibers with (a) 250 μm, (b) 500 μm, (c) 1 mm, and (d) 1.5 mm diameters.

To suppress high-order modes in HCFs with larger cores, we also studied the effect of using a gas pressure-gradient and inducing a chirp in the input pulse, both of which can be used to mitigate ionization at the fiber inlet. For the gas pressure-gradient method, the pressure was gradually increased with the propagation distance according to $p(x) = \sqrt{p_{\rm in}^2 + x(p_{\rm out}^2 - p_{\rm out}^2)/L}$,[27] where $p_{\rm in}$ and $p_{\rm out}$ are the gas pressures at the fiber inlet and outlet, respectively; L is the fiber length; and x is the propagation distance. $p_{\rm in}$ was set to be 2 mbar, which corresponds to the lowest pressure obtained by the pump in our lab. $p_{\rm out}$ was set to be 450 mbar. Thus, the accumulated nonlinearity $\int_0^L n_2 {\rm d}z$ for the pressure gradient implementation was the same as that for the 300 mbar static pressure case. Figure 4(a) shows the evolution of the normalized pulse energies of different fiber modes in the 1 mm HCFs filled with gradient-pressure argon. The other parameters are the same as those in Fig. 1(c). It can be seen that the low pressure at the input prevents the excitation of high-order modes. However, as the pressure increases, the beam quality deteriorates quickly. After 1 m propagation, the mode energy distribution is almost the same as that in the static pressure case. This indicates that the pressure gradient method will not improve the beam quality in large-core HCFs.

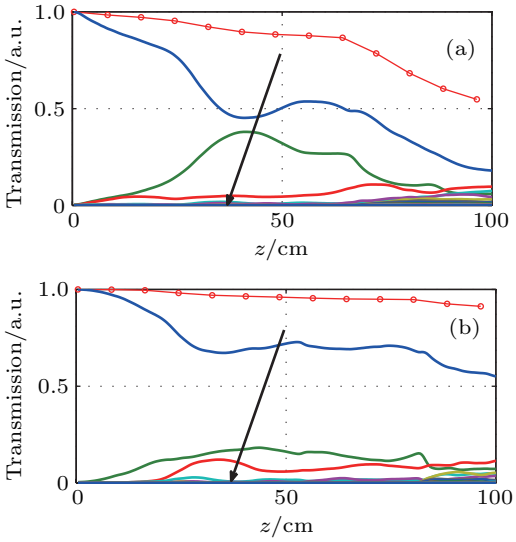

Fig. 4. (color online) Evolutions of normalized energies of the pulse (red-dotted lines) and different fiber modes (solid lines with various colors represent different fiber mode orders m of Eq. (1)) in the hollow-core fibers with 1 mm diameters. (a) The gas pressure increases from 2 mbar to 450 mbar; (b) the input pulse is positively chirped to 100 fs.

In the second method, the original 40 fs FWHM pulse was stretched by a positive chirp to 100 fs, thus decreasing the

peak power. This reduces the self-focusing effect. Figure 4(b) shows the evolution of the normalized chirped pulse energies of different fiber modes in the 1 mm HCF. The Q factor increases to more than 0.6 after 1 m propagation. The overall transmission is also improved significantly. Therefore, it is the peak power of the pulse that determines the beam quality in large-core HCFs.

4. Discussion

In the past decade, the need for few-cycle intense pulses at longer wavelengths has grown. As the wavelength increases, the nonlinear refractive index n_2 becomes smaller; the ionization rate also decreases and the mode discrimination effect becomes larger. Therefore, HCFs with larger cores are more suitable for longer wavelength pulses. We conducted simulations of the propagation dynamics of pulses at 1.8 μm with the same peak intensity at the fiber inlet and gas pressure used in Fig. 1. Figure 5 shows the Q factors in different HCFs after 1 m propagation, compared with those of the 800 nm pulses. The beam quality of the 1800 nm pulse is better than that of the 800 nm pulse in the same HCF. It is also clear that, as the diameter increases, the Q factor approaches a lower limit.

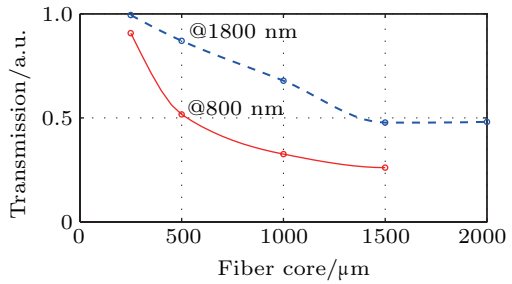

Fig. 5. (color online) The ratios of the fundamental mode energy to the pulse energy after 1 m propagation in HCFs with different inner diameters.

Finally, we discuss scale-invariant propagation in HCFs. Basically, this is the scaling of the HCF inner diameter. As mentioned in the introduction, the main obstacle to linear scaling is the nonlinear dependence of waveguide attenuation on the fiber inner diameter. Additionally, the fiber length is at most 3 m. Thus, scaling the inner diameter is limited to a small range. For example, if the fiber length is increased from 1 m to 3 m, the inner diameter should be increased by $\sqrt[3]{3}$ times (~ 1.4 times) to scale the waveguide attenuation term in Eq. (1). To circumvent this problem, a wavelength parameter can be introduced into the scaling factor set along with the geometrical parameters and gas density. Unfortunately, the plasma effect in Eq. (1) has a nonlinear dependence on the wavelength. However, if the plasma effect is negligible, it is possible to achieve scale-invariant propagation in HCFs over a large range of inner diameters. This requires further study.

5. Conclusion

We performed a numerical study of the nonlinear propagation of intense optical pulses in gas-filled HCFs of different inner diameters. When the input peak intensity is kept the same, the spatiotemporal dynamics of the pulses exhibit a transition from tightly confined to loosely confined characteristics as the fiber core increases, a result of the increase in pulse peak power. In the loosely confined waveguide, more than five modes are excited to a significant level due to the self-focusing effect, and the pulse envelope splits in both the temporal and spatial domains. The gas pressure-gradient method does not improve the beam quality in large-core HCFs, while inducing a positive chirp in the pulse leads to some improvement. Large-core HCFs are also found to support high pulse energies at longer wavelengths with good beam quality. These results will benefit the generation of energetic few-cycle pulses in large-core HCFs.

References

[1] Brabec T and Krausz F 2000 *Rev. Mod. Phys.* **72** 545
[2] Krausz F and Ivanov M 2009 *Rev. Mod. Phys.* **81** 163
[3] Nisoli M, Silvestri S D and Svelto O 1996 *Appl. Phys. Lett.* **68** 2793
[4] Suda A, Hatayama M, Nagasaka K and Midorikawa K 2005 *Appl. Phys. Lett.* **86** 111116
[5] Chen X W, Zou J P, Martin L, Simon F, Martens R L and Audebert P 2009 *Opt. Lett.* **34** 1588
[6] Bohman S, Suda A, Kanai T, Yamaguchi S and Midorikawa S 2010 *Opt. Lett.* **35** 1887
[7] Mashiko H, Nakamura C M, Li C, Moon E, Wang H, Tackett J and Chang Z 2007 *Appl. Phys. Lett.* **90** 161114
[8] Arnold C L, Zhou B, Akturk S, Chen S, Couairon A and Mysyrowicz A 2010 *New J. Phys.* **12** 073015
[9] Wang D, Leng Y X and Xu Z Z 2012 *Opt. Commun.* **285** 2418
[10] Wang D, Leng Y X and Huang Z Y 2014 *J. Opt. Soc. Am. B* **31** 1248
[11] Jacqmin H, Jullien A, Mercier B, Hanna M, Druon F, Papadopoulos D and Lopez-Martens R 2015 *Opt. Lett.* **40** 709
[12] Cardin V, Thire N, Beaulieu S, Wanie V, Legare F and Schmidt B E 2015 *Appl. Phys. Lett.* **107** 181101
[13] Vozzi C, Nisoli M, Sansone G, Stagira S and Silvestri S De 2005 *Appl. Phys. B* **80** 285
[14] Tempea G and Brabec T 1998 *Opt. Lett.* **23** 762
[15] Braun A, Korn G, Liu X, Du D, Squier J and Mourou G 1995 *Opt. Lett.* **20** 73
[16] Adachi S, Ishii N, Nomura Y, Kobayashi Y, Itatani J, Kanai T and Watanabe S 2010 *Opt. Lett.* **35** 980
[17] Herrmann D, Veisz L, Tautz R, Tavella F, Schmid K, Pervak V and Krauze F 2009 *Opt. Lett.* **34** 2459
[18] Granados E, Chen L, Lai C, Hong K and Kaertner F X 2012 *Opt. Express* **20** 9099
[19] Hely C M, Coudert-Alteirac H, Miranda M, Louisy M, Kovacs K, Tosa V, Balogh E, Varju K, L'Huillier A, Couairon A and Arnold C L 2016 *Optica* **3** 75
[20] Hauri C P, Kornelis W, Helbing F W, Heinrich A, Couairon A, Mysyrowicz A, Biegert J and Keller U 2004 *Appl. Phys. B* **79** 673
[21] Mechain G, D'Amico C, Andre Y B, Tzortzakis S, Franco M, Prade B, Mysyrowicz A, Couairon A, Salmon E and Sauerbrey R 2005 *Opt. Commun.* **247** 171
[22] Kolesik M and Moloney J V 2004 *Phys. Rev. E* **70** 036604
[23] Marcatili E A and Schmeltzer R A 1964 *Bell Syst. Tech. J.* **43** 1783
[24] Perelomov A M, Popov V S and Terent'ev M V 1966 *Sov. Phys. JETP* **23** 924
[25] Ammosov M V, Delone N B and Krainov V P 1986 *Sov. Phys. JETP* **64** 1191
[26] Hassan H Th, Wirth A, Grguras I, Moulet A, Luu T T, Gagnon J, Pervak V and Goulielmakis E 2012 *Rev. Sci. Instrum.* **83** 111301
[27] Nurhuda M, Suda A, Midorikawa K, Hatayama M and Nagasaka K 2003 *J. Opt. Soc. Am. B* **20** 2002